Mouse model of hemolytic-uremic syndrome caused by endotoxin-free Shiga toxin 2 (Stx2) and protection from lethal outcome by anti-Stx2 antibody

Mouse Model of Hemolytic-Uremic Syndrome Caused by Endotoxin-Free Shiga Toxin 2 (Stx2) and Protection from Lethal Outcome by Anti-Stx2 Antibody

Kristin A. D. Sauter, Angela R. Melton-Celsa, Kay Larkin, Megan L. Troxell, Alison D. O'Brien and Bruce E. Magun
Infect. Immun. **2008, 76(10):4469. DOI: 10.1128/IAI.00592-08. Published Ahead of Print 11 August 2008.**

INFECTION AND IMMUNITY, Oct. 2008, p. 4469–4478 Vol. 76, No. 10
0019-9567/08/$08.00+0 doi:10.1128/IAI.00592-08

Mouse Model of Hemolytic-Uremic Syndrome Caused by Endotoxin-Free Shiga Toxin 2 (Stx2) and Protection from Lethal Outcome by Anti-Stx2 Antibody▽

Kristin A. D. Sauter,[1] Angela R. Melton-Celsa,[2] Kay Larkin,[3] Megan L. Troxell,[3] Alison D. O'Brien,[2] and Bruce E. Magun[1]*

Department of Cell and Developmental Biology, Oregon Health and Science University, Portland, Oregon 97239[1]; Department of Microbiology and Immunology, Uniformed Services University of the Health Sciences, Bethesda, Maryland 20814[2]; and Department of Pathology, Oregon Health and Science University, Portland, Oregon 97239[3]

Received 14 May 2008/Returned for modification 16 June 2008/Accepted 25 July 2008

Hemolytic-uremic syndrome (HUS) results from infection by Shiga toxin (Stx)-producing *Escherichia coli* and is the most common cause of acute renal failure in children. We have developed a mouse model of HUS by administering endotoxin-free Stx2 in multiple doses over 7 to 8 days. At sacrifice, moribund animals demonstrated signs of HUS: increased blood urea nitrogen and serum creatinine levels, proteinuria, deposition of fibrin(ogen), glomerular endothelial damage, hemolysis, leukocytopenia, and neutrophilia. Increased expression of proinflammatory chemokines and cytokines in the sera of Stx2-treated mice indicated a systemic inflammatory response. Currently, specific therapeutics for HUS are lacking, and therapy for patients is primarily supportive. Mice that received 11E10, a monoclonal anti-Stx2 antibody, 4 days after starting injections of Stx2 recovered fully, displaying normal renal function and normal levels of neutrophils and lymphocytes. In addition, these mice showed decreased fibrin(ogen) deposition and expression of proinflammatory mediators compared to those of Stx2-treated mice in the absence of antibody. These results indicate that, when performed during progression of HUS, passive immunization of mice with anti-Stx2 antibody prevented the lethal effects of Stx2.

Hemolytic-uremic syndrome (HUS) results from infection by Shiga toxin (Stx)-producing *Escherichia coli* (STEC), most commonly serotype O157:H7, and is the most common cause of acute renal failure in children (for reviews, see references 15, 40, 42, and 46). Accumulated evidence points to endothelial cell damage as the hallmark of HUS-associated thrombotic microangiopathy, which is characterized by fibrin deposition within small vessels, swelling of glomerular endothelial cells, and thrombotic occlusion of capillaries (17). Severe cases of HUS exhibit renal cortical necrosis, pervasive inflammatory cell infiltrates in the kidney, and apoptosis of renal and cortical glomerular and tubular cells (20, 23, 55, 62).

STEC expresses either Stx1 or Stx2, which is usually encoded by bacteriophages. Each Shiga holotoxin consists of one A and five B subunits. The B subunit binds to cells via glycosphingolipid receptors such as globotriaosyl ceramide (Gb3), while the A subunit contains N-glycosidase activity (5, 30). Following endocytosis and retrograde transport through the Golgi apparatus, the A subunit enters the cytosol. There, it depurinates a single adenine (A4256 in mice) in a conserved region of the 28S rRNA, thereby inhibiting protein synthesis (9, 10, 36, 49) and simultaneously activating the stress-activated protein kinases (SAPKs) Jun N-terminal kinase (JNK) and p38 (4, 13, 53). Stxs and ricin, a related ribotoxin, induce the release of proinflammatory cytokines and activate the transcription of genes that encode them (27, 37, 40, 43, 48). Activation of SAPKs by Stx and ricin has been tied to their proinflammatory effects (4, 27).

Although administration of intravenous Stx to primates has been able to reproduce the features of HUS (52), the development of an HUS model in small animals has been less successful (2, 44). The inability of Stx to reproduce glomerulopathy in animal models may be due to the variable distribution of receptors for Stx among species (29). In view of the availability of mice containing null mutations in a variety of proinflammatory and regulatory genes, a mouse model of HUS using Stx alone that reproduces the manifestations of human disease would be valuable. The primary impediment to the development of a murine model of HUS has been the inability of investigators to produce glomerular thrombotic microangiopathy (TMA), which is a hallmark of human HUS. Bacterial endotoxin, or lipopolysaccharide (LPS), has been employed in combination with Stx2 to reproduce the signs of HUS (3, 22, 24). However, LPS has been shown to either reduce or enhance Stx toxicity, depending on the time and dose of administration (38). For example, pretreatment with LPS protects animals from the effects of Stx, whereas LPS administered 8 or 24 h but not 0 or 72 h after challenge with Stx enhances the toxicity (3). Mortality rates and cytokine production in mice remained unchanged after administration of various concentrations of Stx in combination with sublethal doses of LPS at various times (54). Ikeda et al. found that LPS, when administered at the appropriate time, was essential for induction of HUS; however, this model lacked the typical hemolytic anemia. (19). Keepers et al. developed another murine model using Stx and LPS; however, some of the signs, such as lym-

* Corresponding author. Mailing address: Department of Cell and Developmental Biology, Oregon Health and Science University, 3181 SW Sam Jackson Park Rd., Portland, OR 97239. Phone: (503) 494-7811. Fax: (503) 494-4253. E-mail: magunb@ohsu.edu.

▽ Published ahead of print on 11 August 2008.

phocytopenia and neutrophilia, were transient, lasting only a few hours (24).

Currently, specific therapeutics for HUS are lacking, and therapy for HUS patients is primarily supportive. Although diagnostic reagents have recently been developed for early detection of Stx (57), and antibodies (Abs) (chimeric, humanized, and fully human) have been developed for potential passive immunization (6, 8, 28, 34, 35), it is unclear whether administration of anti-Stx therapeutics would be effective when performed after signs have developed in humans, though these Abs are protective after infection with STEC in a mouse model of infection (50, 64). Stx that is bound to polymorphonuclear leukocytes was detected for up to 1 week after diagnosis in the circulation of patients who had developed HUS (58). This suggests that delayed delivery of toxin to the microvasculature over an extended time may contribute to the clinical signs of HUS (58). For these reasons, passive immunization with anti-Stx2 Ab following the appearance of initial signs may block the development of clinical signs and alleviate disease in patients who have been diagnosed with HUS (60).

In the present studies, we have developed a model of HUS in mice by administering multiple sublethal doses of Stx2, in the absence of LPS, over a period of 7 to 8 days. Administration of a mouse monoclonal Ab (11E10) directed against Stx2 was able to halt the lethality and reverse the manifestations of HUS when Ab was delivered as late as 4 days after the initial exposure to Stx2. These data suggest that, in this model of murine HUS, Stx2-mediated renal failure required extended exposure and that administration of anti-Stx2 Ab midway through the course of administration interfered with an otherwise lethal outcome.

MATERIALS AND METHODS

Mice. C57BL/6J mice were purchased from The Jackson Laboratory, Bar Harbor, ME. Male mice aged 8 to 10 weeks of age and weighing 18 to 24 g were used throughout the experiments. Mice were housed under a 12-hour light-dark cycle and fed a standard diet ad libitum. Groups of mice were injected intraperitoneally with 50 μl of either saline, Stx2, or Stx2 plus 11E10 antibody as follows: (i) saline (control solvent) on days 0, 3, and 6; (ii) 5 ng Stx2/20 g of body weight (bwt) on day 0; (iii) 1 ng Stx2/20 g bwt on days 0, 3, and 6; or (iv) 1 ng Stx2/20 g bwt on days 0, 3, and 6 plus 30 ng 11E10 Ab/20 g bwt on day 4. Mice were weighed on day 0 and every day thereafter. To collect 24-hour urine, mice were housed for 24 to 48 h in "diuresis metabolic cages" (model M-D-METAB; Nalgene, Braintree, MA) and provided with a ground standard diet ad libitum. Before experimental procedures, mice were anesthetized intraperitoneally with 80 mg ketamine/kg of body weight and 10 mg/kg xylazine. All of the animal procedures were performed according to protocols that have been approved by the Institutional Animal Care and Use Committee at Oregon Health and Science University, Portland, OR.

Reagents and Abs. The mouse monoclonal anti-Stx2 Ab (11E10) has been previously described (41). Ab against fibrin/fibrinogen (YNGMFbg7S) was purchased from Accurate Chemical and Scientific (Westbury, NY). Stx2 was produced in *E. coli* DH5 using the pLPSH3 plasmid and purified by immunoaffinity chromatography as previously described (33). When examined by sodium dodecyl sulfate-polyacrylamide gel electrophoresis (SDS-PAGE), the toxin preparation exhibited the expected bands representing the A, A1, and B subunits. In addition, the specific activity of the toxin for Vero cells was 1×10^7 50% cytotoxic doses per μg. Stx2 was dissolved in 0.9% endotoxin-free saline (Braun Medical Inc.). Levels of endotoxin were undetectable, as determined with a *Limulus* amebocyte assay (Cambrex).

Mouse blood studies. All blood analyses were performed by IDEXX Laboratories (Portland, OR). Mice were euthanized, and blood was collected. Whole blood for cell count analysis and cell type determination was collected in hematology tubes with tripotassium EDTA (Microtainer; Becton Dickinson, Franklin Lakes, NJ). In addition, total blood was left to coagulate at room temperature for 10 min, after which samples were centrifuged at 8,000 rpm and 4°C for 10 min and serum was collected. Biochemical determinations of blood urea nitrogen (BUN) and serum creatinine levels were performed.

Proteinuria studies. Mice were housed in "diuresis metabolic cages" for 24 to 48 h, during which time urine was collected. Equal amounts of urine from each mouse were further concentrated through 30-kDa Micropore concentration tubes. Urine samples were mixed 1:2 with 4× SDS-PAGE loading buffer and boiled at 95°C for 5 min. Samples from each group of three mice were pooled and separated via 10% SDS-PAGE. Gels were stained with Gelcode Blue staining solution. Bovine serum albumin was loaded on the same gel as a positive control.

Spectrophotometric determination of hemoglobin levels in serum. Total blood was left to coagulate at room temperature for 10 min, after which samples were centrifuged at 8,000 rpm and 4°C for 10 min. Two microliters of serum was used to obtain an absorption spectrum in a Nano Drop spectrophotometer (Nano Drop, Wilmington, DE).

Immunohistochemistry. Mice were anesthetized and sacrificed by cervical dislocation. The kidneys were dissected, fixed in Carnoy solution for 2 h, and transferred to 70% ethanol. The organs were embedded in paraffin blocks and sectioned into 5-μm sections. After blocking in serum, the slides were incubated with primary Abs overnight at 4°C at appropriate dilutions. Slides were further processed using the VectaStain Elite ABC kit (Vector Laboratories, Burlingame, CA) according to the manufacturer's recommendations using 3,3′-diaminobenzidine as substrate. Photomicrographs of immunohistochemical preparations in Fig. 2A and 7A were taken at a ×1,000 magnification at identical exposure times.

Detection of tissue fibrin(ogen) by immunoblotting. Fibrin(ogen) deposition in kidneys was detected as described previously (63). Frozen kidneys were homogenized in 10 mM sodium phosphate buffer (pH 7.5) containing 5 mM EDTA, 100 mM ε-aminocaproic acid, 10 U/ml heparin, and 2 mM phenylmethylsulfonyl fluoride. The homogenate was incubated for 18 h on a top-over-top rotor at 4°C. After centrifugation (10,000 rpm, 4°C, 10 min), the pellet was resuspended in the same 10 mM sodium phosphate buffer as above, without phenylmethylsulfonyl fluoride, and recentrifuged. Pellets were resuspended in 3 M urea, agitated for 2 h at 37°C, and centrifuged at 14,000 rpm at 4°C for 15 min. The pellets were resuspended in reducing SDS sample buffer (10 mM Tris [pH 7.5], 5% glycerol, 2% SDS, 5% β-mercaptoethanol, and 0.4 mg/ml bromophenol blue) and dissolved at 65°C for 90 min with vortexing every 15 min. Samples were subjected to SDS-PAGE (7.5%; 5% stacking gel) and transferred to a polyvinylidene difluoride membrane. Fibrin chains were detected with a fibrin(ogen) Ab and a chemiluminescence system. Fibrin standards were prepared by clotting a known amount of rat fibrinogen (Sigma) with an excess of human thrombin (Sigma) at 37°C for 10 min. After 2× SDS sample buffer was added, the standards were incubated at 65°C for 90 min.

Electron microscopy. After dissection of the kidneys, tissue was fixed and processed using standard procedures, including immediate fixation in 2.5% glutaraldehyde in sodium phosphate buffer for 2 hours, postfixation in osmium tetroxide, and embedding in plastic resin. Thick sections (1 μm) were stained with toluidine blue, and ultrathin sections were stained with uranyl acetate and lead citrate. Photomicrographs were taken at ×11,000 magnification.

RNA isolation. After dissection of the kidneys, the tissue was immediately frozen and ground in liquid nitrogen. RNA was extracted using TRIzol reagent in accordance with the manufacturer's instructions and was further digested with DNase. Both reagents were purchased from Invitrogen Life Technologies, Carlsbad, CA.

Real-time PCR analysis. Two micrograms of RNA was reverse transcribed in the presence of SuperScript II and oligo(dT) primers (both reagents were purchased from Invitrogen Life Technologies). The amplification of the cDNA was accomplished in an ABI Prism 7900HT sequence detection system (Applied Biosystems, Foster City, CA) in the presence of the commercially available Sybr green PCR Master Mix (Applied Biosystems) and 20 μmol/liter of the corresponding sense and antisense reverse transcription-PCR (RT-PCR) primers for 120-bp amplicons in a 40-cycle PCR. Each sample was analyzed in triplicate. Induction in gene expression was measured using absolute quantitation of a standard curve in arbitrary units. The denaturing, annealing, and extension conditions of each PCR cycle were 95° for 15 s, 55° for 30 s, and 72° for 30 s, respectively. The SDS software was used for normalization of the raw data. The nucleotide sequences of primers used in this study have been previously published (28).

Reverse transcription of rRNA by primer extension. Reverse transcription of rRNA was performed as described by Iordanov and colleagues (21). The oligonucleotide primer 5′-CACATACACCAAATGTC-3′ (Invitrogen Life Technologies) was end labeled with T4 polynucleotide kinase (Life Technologies, Inc.). A 10-μl mixture of 2 μg total RNA and 1.0 pmol primer in 50 mmol/liter

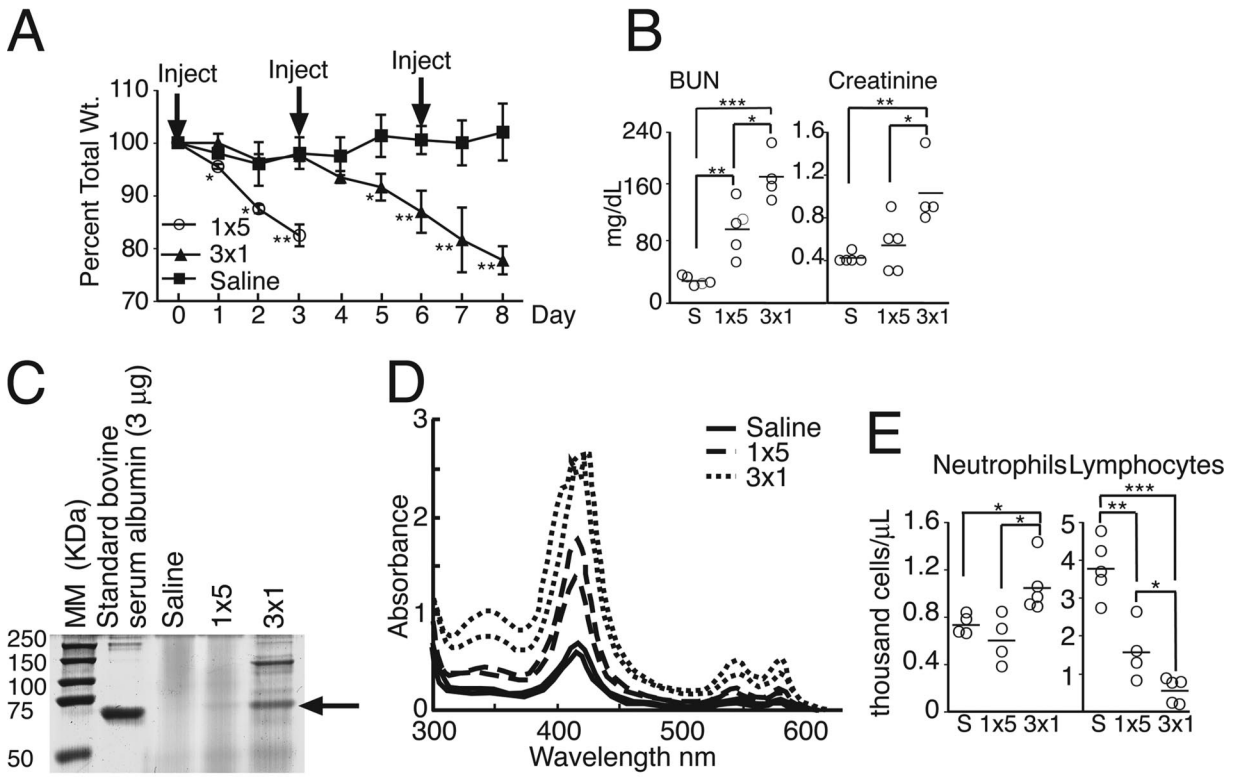

FIG. 1. Analysis of bwt, blood parameters, and urine after administration of Stx2 to mice. Groups of mice were injected with Stx2 or saline as follows: (i) 1x5, a single injection of 5 ng Stx2/20 g bwt at $t = 0$; (ii) 3x1, three injections of 1 ng Stx2/20 g bwt at $t = 0$, $t = 3$ days, and $t = 6$ days; and (iii) saline (S), three injections of 50 μl saline at $t = 0$, $t = 3$ days, and $t = 6$ days. (A) Percent total bwt loss in mice injected with Stx2 or saline. Mouse weight at day 0 was set at 100%. Data reflect five mice per group ± standard deviations. *, $P < 0.05$; **, $P < 0.01$. (B) Measurement of BUN and creatinine levels in sera. Each circle represents the measurement of BUN or creatinine level from one mouse; black bars represent the means of samples in each group. Brackets indicate levels of significance between groups: *, $P < 0.05$; **, $P < 0.01$; ***, $P < 0.001$. (C) Presence of protein in urine of mice following administration of Stx2 or saline. Equal amounts of pooled urine from groups of three saline-injected, 1x5, and 3x1 mice were separated by SDS-PAGE. Bovine serum albumin (3 μg) was used as a standard for albumin. MM, molecular mass. (D) Measurement of hemoglobin by absorption spectrophotometry of sera. Absorption spectrophotometry of sera from two saline-injected, 1x5, and 3x1 mice demonstrate absorbance maxima at 430 nm and 575 nm, characteristic of hemoglobin. (E) Measurement of neutrophil and lymphocyte numbers. Each circle represents the measurement of neutrophil or lymphocyte numbers from one mouse; black bars represent the means of samples in each group. Brackets indicate levels of significance between groups: *, $P < 0.05$; **, $P < 0.01$; ***, $P < 0.001$.

Tris-HCl (pH 8.3)–75 mmol/liter KCl–3 mmol/liter $MgCl_2$ was incubated at 90°C for 3 min and then placed on ice for 5 min, followed by an incubation at room temperature for 5 min. The reverse transcription was initiated by the addition of 10 μl of a mixture of 2 mmol/liter deoxynucleoside triphosphates and 30 U SuperScript (Life Technologies, Inc.) in 50 mmol/liter Tris-HCl (pH 8.3), 75 mmol/liter KCl, 3 mmol/liter $MgCl_2$, 10 mmol/liter dithiothreitol, followed by an incubation at 48°C for 15 min, when the reactions were stopped by the addition of 5 mmol/liter EDTA. Reaction products were precipitated in ethanol, resuspended in formamide gel loading buffer, heat denatured, and electrophoresed in an 8% acrylamide sequencing gel, which was subsequently dried and exposed to a PhosphorImager screen.

Multiplex cytokine detection. Serum samples were analyzed using a customized multiplex mouse cytokine kit from Linco Research (St. Charles, MO) and detected on the LiquiChip workstation (Qiagen, Valencia, CA). Each sample was analyzed in duplicate.

Statistical analysis. Individual groups were compared using unpaired *t* test analysis. To estimate *P* values, all statistical analyses were interpreted in a two-tailed manner. *P* values of <0.05 were considered statistically significant.

RESULTS

To examine the consequences of Stx2 administered intraperitoneally to C57BL/6J mice, we first determined the toxicity of Stx2 when administered as a single dose. Dose-response experiments determined that the 50% lethal dose was 3 ng Stx2/20 g bwt (data not shown). In initial experiments, administration of a lethal dose of Stx2 (a single dose of 5 ng Stx2/20 g bwt, hereafter referred to as "1x5") resulted in weight loss detected 24 h later, which continued for 3 days (Fig. 1A). At that time, animals were moribund, having lost at least 20% of their bwt and displaying tremors and ataxia. For ethical reasons, these mice were euthanized on the third day following injection of Stx2. BUN levels from these animals increased from 31 ± 6.3 to 103.8 ± 36.6 mg/dl ($P < 0.05$), but creatinine levels failed to differ significantly (Fig. 1B). Urine from these animals failed to show signs of albuminuria, an indicator of renal failure, as determined by PAGE (Fig. 1C). The presence of hemoglobin in serum was evaluated by determining the absorbance spectrum of serum. Mice receiving 1x5 Stx2 showed an increased spectral absorbance profile characteristic of free hemoglobin (7) (Fig. 1D). Animals receiving 1x5 Stx2 failed to show an increase in circulating neutrophils, although they exhibited a significant decrease in circulating lymphocytes (Fig. 1E). From these data, we concluded that administration

of 1x5 Stx2 triggered some hemolysis and a modest impairment of renal function, as evidenced by increased BUN levels, but failed to induce other significant signs of renal dysfunction, such as increased creatinine and proteinuria levels.

Signs of HUS in humans usually do not appear earlier than 1 week following exposure to STEC (60). We considered, therefore, that mice may require an extended time interval between initial exposure to Stx2 and the development of signs of HUS. First, we investigated whether lower doses of Stx2 that allowed mice to survive for at least 1 week would permit the animals to develop more-severe manifestations of HUS, including renal failure. However, single doses of Stx2 lower than 5 ng/20 g bwt that permitted animals to survive more than 3 days were ineffective in inducing either toxicity or signs of renal failure (not shown). We then tested whether administration of successive, lower doses of Stx2 over an extended time course would permit the animals to develop signs characteristic of HUS in humans. When we administered two injections of 1 ng Stx2/20 g bwt (at days 0 and 3), mice showed minor signs of toxicity and renal failure when sacrificed 8 days later (data not shown). We then injected animals with three doses of 1 ng Stx2/20 g bwt at day 0, day 3, and day 6 (hereafter referred to as "3x1"). The mice receiving 3x1 Stx2 did not begin to lose significant bwt until day 5 (Fig. 1A). By day 7 or 8, these mice had lost a total of 20 to 25% of their initial bwt and were euthanized. Unlike mice receiving 1x5 Stx2, these animals did not exhibit neurological signs at time of sacrifice. BUN levels increased nearly sixfold ($P < 0.001$) in the 3x1 Stx2 mice, while creatinine levels increased 2.5-fold ($P < 0.01$) compared to those of saline-injected control mice (Fig. 1B). The urine of the 3x1 Stx2 mice displayed increased protein content with a major protein band corresponding in size to serum albumin and additional bands of proteins with higher molecular weight (Fig. 1C). The increased serum levels of BUN and creatinine and the appearance of proteinuria suggested that administration of 3x1 Stx2 resulted in compromised renal function. Furthermore, spectrophotometric analysis of serum from these mice revealed hemolysis, as evidenced by levels of hemoglobin in the serum that were greater than that seen in 1x5 animals (Fig. 1D). Unlike the 1x5 mice, the 3x1 mice exposed for 7 to 8 days developed increased numbers of circulating neutrophils (from 738.8 ± 83.1 cells/μl in control mice to 1,047.6 ± 223.8 cells/ml in Stx2-treated mice [$P < 0.05$]) and decreased numbers of lymphocytes (from 3,779.6 ± 767.1 cells/ml in control mice to 566 ± 327.9 cells/ml in Stx2-treated mice [$P < 0.001$]) (Fig. 1E).

Glomerular TMA is a distinguishing feature of human HUS that has been difficult to recreate in animal models. Compared with those from animals treated with saline, kidneys from mice receiving 1x5 Stx2 showed a small amount of fibrin(ogen) deposition in glomerular vessels, as demonstrated by both antifibrin(ogen) immunohistochemistry (Fig. 2A) and immunoblotting (Fig. 2B). However, mice injected with 3x1 Stx2 demonstrated abundant deposition of fibrin(ogen) in the glomerular capillary loops, with some capillaries appearing to be completely occluded (Fig. 2A). The deposition of increased fibrin(ogen) in kidneys from these mice was confirmed by immunoblotting (Fig. 2B). Transmission electron microscopy of kidneys from two 3x1 Stx2 animals revealed enlarged subendothelial zones (asterisk, Fig. 3B) containing flocculent material (so called subendothelial "fluff") with accompanying endothelial cell cytoplasmic swelling and loss of fenestrae (area delimited by bracket). Subtle mesangiolysis was also seen focally (data not shown). Kidneys from 1x5 Stx2-treated animals showed similar but less pronounced alterations in morphology of glomeruli (data not shown).

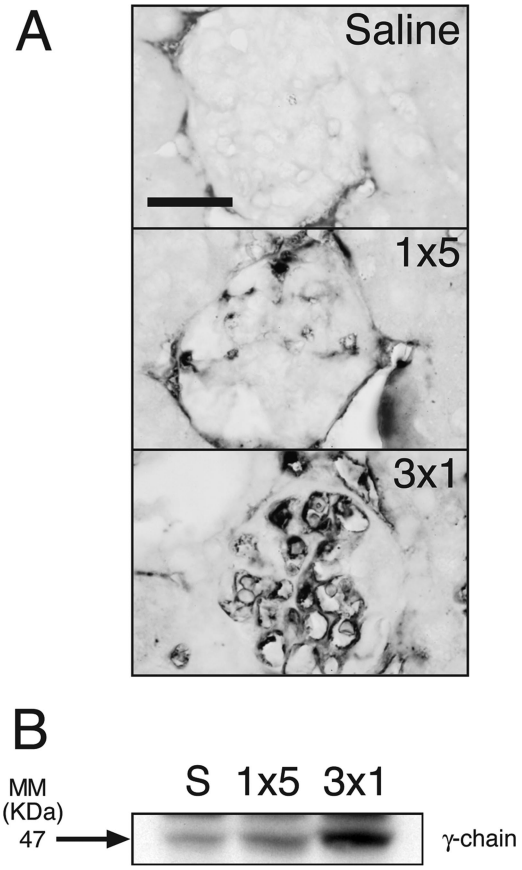

FIG. 2. Detection of fibrin/fibrinogen by immunohistochemistry and immunoblotting. Groups of five mice were injected with Stx2 or saline as described for Fig. 1. From each mouse, one half-kidney was fixed and embedded for immunohistochemistry and the other half was homogenized in lysis buffer for immunoblotting. Immunohistochemistry and immunoblotting were performed on each kidney specimen. (A) Immunohistochemical detection of fibrin/fibrinogen. The photomicrograph displayed in this figure is representative of immunohistochemical reactivity. Bar, 20 μm. (B) Detection of fibrin/fibrinogen by immunoblotting. The volume of lysis buffer employed for extraction was adjusted for the weight of each half-kidney. Following preparation of the lysate, 50 μl was separated by electrophoresis and transferred to a membrane for immunoblotting with antifibrin(ogen) as described in Materials and Methods. The procedure for preparation of kidney lysates has been described in Materials and Methods. The immunoblot in this figure is representative of the five independent lysates that were examined. MM, molecular mass.

Inflammatory responses. We next analyzed RNA from mouse kidneys by real-time RT-PCR, to determine the effects of Stx2 on the expression of mRNA transcripts that encode proteins implicated in inflammatory responses. Groups of five mice injected with 1x5 Stx2 or 3x1 Stx2 were sacrificed on day 3 or day 7, respectively. Animals receiving saline alone were sacrificed on day 7. The transcripts evaluated included cy-

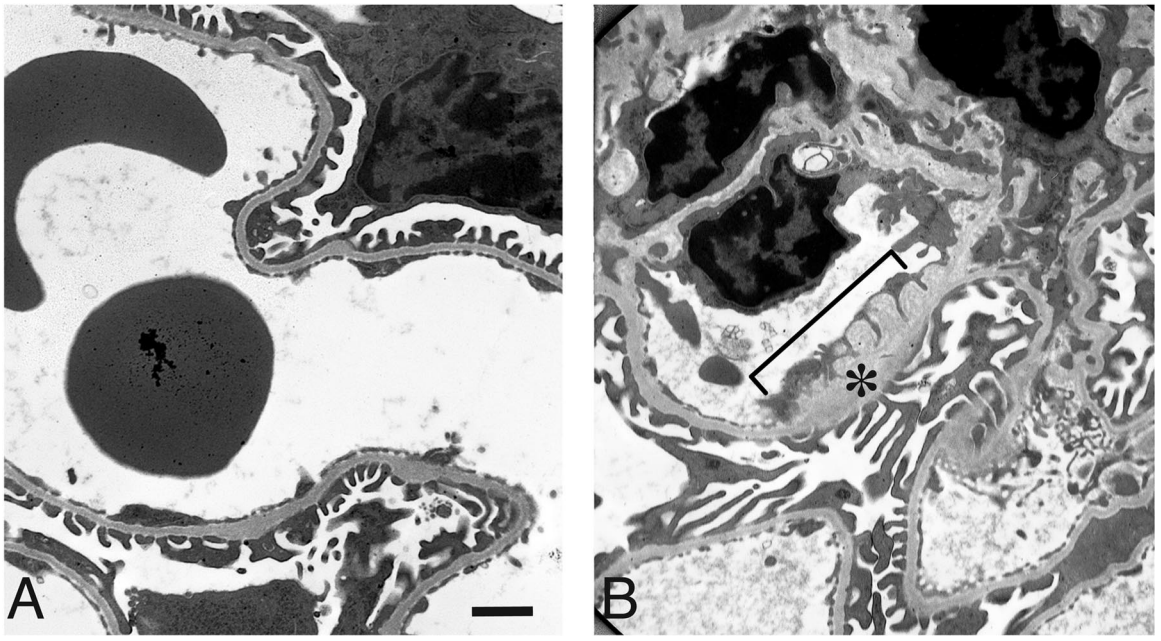

FIG. 3. Transmission electron microscopy of glomeruli from saline-injected (A) and 3x1 (B) mice. Groups of two mice were injected with either Stx2 or saline as described for Fig. 1. The asterisk in panel B indicates enlarged subendothelial space. The bracketed area delimits the portion of endothelium that has lost fenestrae. Bar, 1 μm.

tokines (tumor necrosis factor alpha [TNF-α], interleukin-1α [IL-1α], IL-1β, and IL-6), chemokines (CCL2/monocyte chemoattractant protein 1 and CXCL1/Gro-α), transcription factors (c-Jun, c-Fos, and EGR1), and a surface adhesion protein (intercellular adhesion molecule 1). The results were expressed as increase in RNA expression in Stx2-treated animals over that of saline controls, using glyceraldehyde phosphate dehydrogenase mRNA as a control to standardize the samples (Fig. 4A). The administration of either 1x5 or 3x1 Stx2 significantly elevated the expression of the majority of transcripts investigated. The expression levels of two gene transcripts, CXCL1/Gro-α and IL-6, were significantly greater in the 3x1 Stx2-treated mice than in the 1x5 Stx2-treated mice.

We employed a customized multiplex mouse cytokine kit to measure the expression of several proinflammatory cytokines and chemokines in the serum of mice treated with saline or Stx2. Administration of either 1x5 or 3x1 Stx2 significantly elevated the levels of all proinflammatory proteins investigated compared to those in saline-injected control mice (Fig. 4B). However, levels of these proteins in sera from 1x5 and 3x1 mice did not differ significantly from each other (Fig. 4B). The data shown in Fig. 4B suggest that the Stx2-induced increase in expression of transcripts encoding proinflammatory cytokines and chemokines was associated with an increased level of corresponding proteins in the serum. Importantly, these data indicated that the induced expression of proinflammatory mRNAs associated with Stx2 intoxication resulted in the synthesis of proteins directed by those mRNAs, even in the face of potentially decreased levels of protein synthesis that may occur following Stx2-induced damage to 28S rRNA.

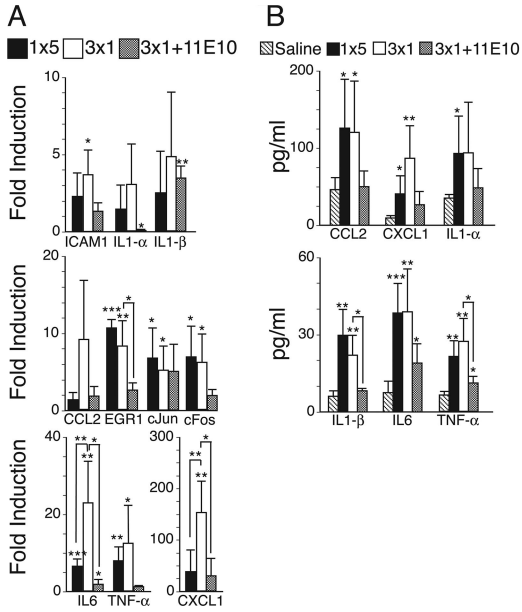

FIG. 4. Measurement of proinflammatory gene products in mouse kidneys and sera. Groups of mice were injected with Stx2 or saline as described for Fig. 1. In addition, a group of 3x1 mice was injected with 11E10 on day 4 (gray bars). (A) Measurement of RNA transcripts by quantitative real-time RT-PCR. Kidney RNA was analyzed from five animals per group (saline, 1x 5, 3x1, or 3x1 plus 11E10). Each bar represents the mean increase in RNA expression ± standard error of the mean compared with values obtained from control saline-injected mice. Brackets indicate levels of significance between groups: *, $P < 0.05$; **, $P < 0.01$; ***, $P < 0.001$. (B) Measurement of cytokines and chemokines in sera from groups of three mice. Sera were analyzed from three animals per group (saline, 1x5, 3 x1, or 3x1 plus 11E10). Each bar represents the mean value of each protein ± standard deviation. Brackets indicate levels of significance between groups: *, $P < 0.05$; **, $P < 0.01$; ***, $P < 0.001$.

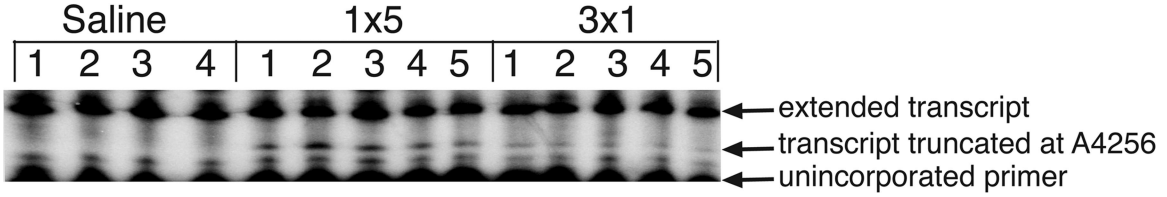

FIG. 5. Detection of lesions at A4256 in 28S rRNA by primer extension. Groups of mice were injected with Stx2 or saline as described for Fig. 1. Total RNA was purified from kidneys of four or five mice per group. Each lane represents a different mouse. Truncated transcripts at A4256 were detected from all Stx2-treated mouse kidneys (middle arrow).

Stx2-mediated lesions in 28S rRNA. Stx2 may impair kidney function by acting directly on cells of the kidney and/or indirectly by inducing the release of inflammatory mediators into the systemic circulation from body tissues. To determine the existence of damage to renal 28S rRNA specifically caused by Stx2, we applied primer extension analysis, a technique that produces truncated radiolabeled transcripts at the site of depurination (A4256) in 28S rRNA (21). RNA extracted from the kidneys of mice exposed to 1x5 Stx2 displayed the strongest lesion-specific signals (Fig. 5). Lesions in A4256 were also observed in the 3x1 Stx2 mice but were diminished in amount compared with lesions produced by 1x5 Stx2. These results indicated that a single dose of 5 ng Stx2 produced more lesions in renal 28S rRNA than did three successive injections of 1 ng Stx2.

Passive immunization by anti-Stx2 Ab. To determine whether administration of anti-Stx2 Ab could prevent progression of HUS in our model, we administered 11E10, a monoclonal Ab, to mice exposed to 3x1 Stx2. For mice receiving three injections of 1 ng Stx2/20 g bwt (on days 0, 3, and 6), we injected a single bolus of 30 ng 11E10 Ab/20 g bwt at different times prior to sacrifice at day 7 to 8. All mice that received Ab on day 4 did not develop subsequent weight loss and appeared normal at time of sacrifice on day 8 (Fig. 6A). However, when Ab was administered to mice on day 5, rescue of some, but not all, mice was achieved (data not shown). Administration of Ab on day 6 failed to rescue any mice (data not shown). To determine whether mice receiving Ab on day 4 would develop impaired kidney function, we evaluated levels of BUN and serum creatinine at day 8 (2 days after mice received the final dose of 1 ng Stx2/20 g bwt). Levels of BUN and serum creatinine in these mice were not different from those in saline-injected control animals (Fig. 6B). In addition, the level of free hemoglobin appearing in sera of 3x1 mice was not increased in the sera of 3x1 Stx2 mice receiving 11E10 Ab on day 4 (Fig. 6C), suggesting that administration of anti-Stx2 Ab to the 3x1 Stx2 mice prevented intravascular hemolysis. The neutrophilia and lymphocytopenia normally present in 3x1 Stx2 mice were not present in 3x1 mice receiving anti-Stx2 Ab on day 4 (Fig. 6D). In addition, the administration of 3x1 Stx2 and 11E10 Ab on day 4 reduced the deposition of fibrin(ogen) in kidneys harvested at 8 days, as determined by both immunohistochemistry and immunoblotting (Fig. 7A and B).

The administration of 11E10 Ab on day 4, in concert with 3x1 Stx2, significantly decreased the expression of the majority of proinflammatory mRNA transcripts that were investigated in the kidneys. Expression of most transcripts decreased by more than 50% compared to kidneys from 3x1 mice that did not receive 11E10 Ab (Fig. 4A). There was also a coordinate decrease in abundance of circulating proinflammatory proteins in sera from these mice compared with mice that had received 3x1 Stx2 alone (Fig. 4B). 3x1 mice receiving 11E10 Ab on day

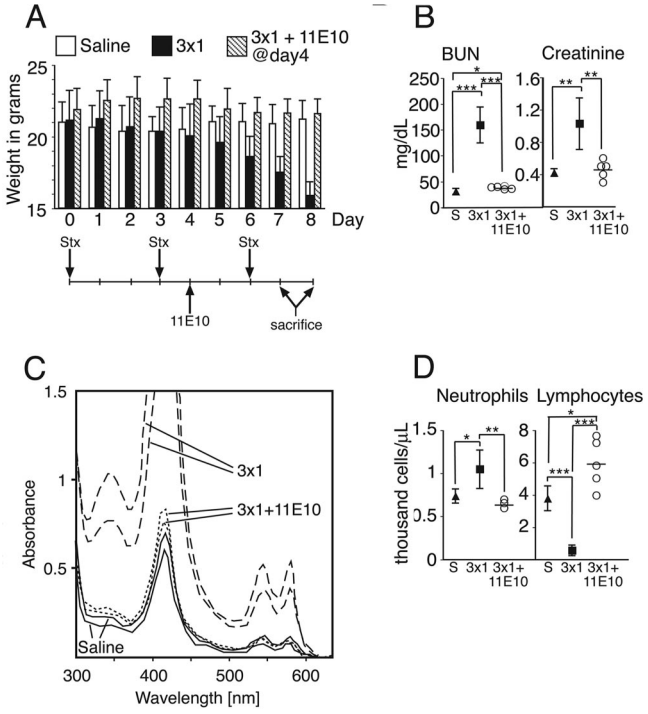

FIG. 6. Analysis of bwt and blood parameters after administration of Stx2 with or without 11E10. Mice received saline, the 3x1 treatment, or the 3x1 treatment plus 11E10 (mouse monoclonal Ab against Stx2) on day 4. (A) Weight loss in mice injected with Stx2 with or without 11E10. Each bar represents the mean value for five mice ± standard deviation. (B) Measurement of BUN and creatinine levels in sera. Data for saline-injected (triangles) and 3x1 (squares) mice have been shown in Fig. 1B; these are included here for comparison with the 3x1 plus 11E10 group. Data are the averages of five mice ± standard deviations. Each circle for 3x1 plus 11E10 represents one mouse; black bars indicate the means of samples for the group. Brackets indicate levels of significance between groups: *, $P < 0.05$; **, $P < 0.01$; ***, $P < 0.001$. (C) Measurement of hemoglobin by absorption spectrophotometry of sera. Absorption spectrophotometry of sera from two saline-injected, 3x1, and 3x1 plus 11E10 mice. (D) Measurement of neutrophil and lymphocyte numbers. Data for saline-injected (triangles) and 3x1 (squares) mice have been shown in Fig. 1E; these are included here for comparison with the 3x1 plus 11E10 group. Data represent the averages of five mice ± standard deviations. Each circle for 3x1 plus 11E10 represents one mouse; black bars indicate the means of samples for the group. Brackets indicate levels of significance between groups: *, $P < 0.05$; **, $P < 0.01$; ***, $P < 0.001$.

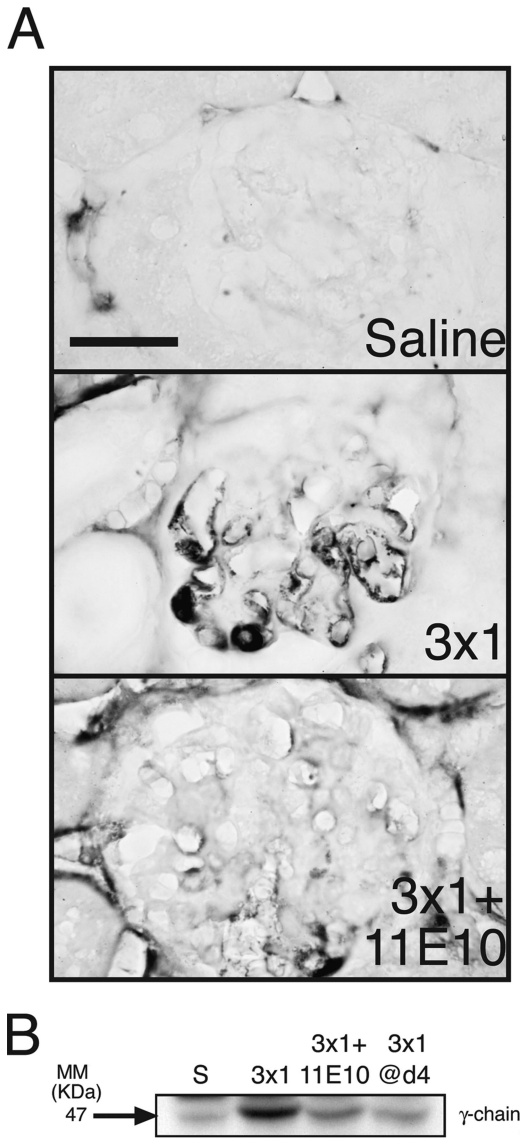

FIG. 7. Detection of fibrin/fibrinogen by immunohistochemistry and immunoblotting after administration of Stx2 with or without 11E10. Groups of mice were injected as described for Fig. 6. (A) Immunohistochemical detection of fibrin/fibrinogen. Bar, 20 μm. (B) Detection of fibrin/fibrinogen by immunoblotting. MM, molecular mass.

4 remained healthy and displayed normal renal function at the time of sacrifice 4 weeks later (data not shown).

DISCUSSION

Stx is the main etiologic factor in the pathogenesis of HUS (40). Although the administration of Stx alone to primates reproduces signs of HUS (52), Stx alone has not been able to produce the majority of HUS signs in small-animal models. The development of a murine model of HUS would provide an economic advantage for therapeutic experimentation and, in view of the ready availability of mouse strains that are deficient in key mediators of inflammatory or coagulatory processes, would further offer the benefit of employing the power of mouse genetics. Although the coadministration of LPS and Stx has been able to reproduce many of the signs of HUS in a murine model (24), these data are controversial because LPS is not required to produce HUS in a primate model (52) and because the required presence of LPS in humans with HUS remains undefined. Furthermore, LPS has been shown to either reduce or enhance Stx toxicity in murine models, depending on the time and dose of administration (38). In this study, we have sought to develop a mouse model of HUS by administering endotoxin-free Stx2.

Administration of a single lethal dose of Stx2 to mice induced hemolysis, lymphocytopenia, and modest impairment of renal function, as evidenced by increased BUN levels at 72 h. Although the lethal dose of Stx2 produced modest renal dysfunction, it was not able to generate many of the significant indicators of renal failure, such as increased creatinine and proteinuria levels. Mice exposed to a single bolus (5 ng/20 g bwt) of Stx2 developed tremors and ataxia prior to death, indicating that the early demise of these mice may have resulted from toxicity for the nervous system. Stx binds to Gb3 receptors in neurons of the central nervous system of mice (26) and has been found to produce brain damage in mice (25). Neurological damage in humans is a frequent complication in HUS (32, 51, 61) and in experimental animals (rabbits) exposed to Stx (14, 56). We reasoned that administration of a lower dose of Stx2 may allow the mice to survive for a longer period of time, permitting them to develop a symptomatic course that would more completely reproduce the characteristics of HUS. Although administration of low doses of Stx2 in a single or double injection was ineffective in producing the array of signs that characterizes HUS, the administration of three successive injections of 1 ng Stx2/20 g bwt at 72-h intervals resulted in the development of many of the manifestations of HUS that develop in humans. The 3x1 mice began losing weight 4 days after the initial injection and, at the time of sacrifice (7 to 8 days), manifested increased BUN, serum creatinine, and proteinuria levels, all of which are indicators of compromised renal function. In addition, these mice developed hemolysis, lymphocytopenia, and neutrophilia, unlike mice that received saline alone. It should be noted that, although analysis of the above indicators was performed at different times in 1x5 mice than in 3x1 mice, the animals at the time of sacrifice had undergone a comparable loss of bwt. Injury of the endothelium contributes to the development of microvascular thrombosis, a common feature of HUS that has been tied to development of renal failure in human patients (40, 42, 43). Endothelial cell injury and thrombosis have been difficult to reproduce in Stx-induced animal models (38, 39, 47, 59). The degree of fibrin(ogen) deposition in glomerular capillaries was greater in 3x1 than in 1x5 mice; some capillaries in the 3x1 mice appeared to be completely occluded (Fig. 2). Furthermore, examination of kidneys from multiply Stx2-injected mice by electron microscopy revealed subtle focal mesangiolysis, subendothelial "fluff," endothelial cell cytoplasmic swelling, and loss of fenestrae. These characteristics are commonly observed in HUS in humans.

Abundant evidence suggests that Stx-induced HUS involves an acute inflammatory response, the magnitude of which is a predictor of clinical outcome. Patients with HUS display markedly elevated levels of proinflammatory cytokines such as

TNF-α and IL-1β and chemokines (45) such as CCL2/monocyte chemoattractant protein 1, CXCL8/IL-8, CXCL1/Gro-α, and CXCL3/Gro-γ (31, 37, 40, 42). Excretion of urinary TNF-α and IL-6 is elevated during the acute phase of HUS in patients (D. Karpman, A. Andreasson, H. Thyssell, B. S. Kaplan, and C. Svanborg, presented at the Second International Symposium and Workshop on Verocytotoxin-Producing *Escherichia coli* Infections, Bergamo, Italy, 1994). Stx has been shown to stimulate the release of proinflammatory cytokines from several types of cultured cells, including macrophages (12), renal podocytes (18), and human vascular endothelial cells (16). Increased expression of proinflammatory transcripts and the presence of proinflammatory chemokines and cytokines in the sera of Stx2-treated mice provided evidence that these animals developed an abundant inflammatory response. At the time of death, expression of circulating proinflammatory mediators was similar in singly and multiply injected mice, suggesting that the development of multiple manifestations of HUS may require an extended exposure to these circulating mediators.

Depurination of a single adenine (A4256 in mice) in a conserved region of the 28S rRNA by Stx is similar to that performed by ricin, a related toxin (11), and is the single known mechanism by which the toxins transduce their signals following entrance into cells (21). This event leads not only to inhibition of protein translation but also to the rapid activation of SAPKs, p38 and JNK, by activating kinases situated upstream in the activating cascade (21, 53). Activation of SAPKs and the subsequent increased production of proinflammatory transcripts occur in the presence of only partial translational inhibition (27). As a consequence, increased levels of transcribed proinflammatory mRNA molecules are capable of being translated into functional proteins (27). Importantly, the present study shows that, similarly to ricin, the Stx2-induced expression of proinflammatory mRNAs resulted in the synthesis of proinflammatory proteins, despite potentially decreased levels of protein synthesis. However, this study does not address whether the cells directly targeted by Stx2 are the ones that secrete the proinflammatory proteins that appear in sera. The increased appearance of proinflammatory proteins may occur secondarily in response to signals initiated in cells that have internalized the Stx2. The 1x5 and 3x1 mice expressed similar levels of proinflammatory transcripts and protein products at their respective times of sacrifice (Fig. 4). However, because analysis of expressed gene products was performed at different times in the two groups (3 days versus 7 to 8 days), the course of expression of mRNA or protein over the exposure interval for each group of mice remains unknown. We postulate that, although 3x1 mice were exposed to a smaller amount of Stx2 than were 1x5 mice, the increased time of exposure over the longer period was responsible in large part for the development of proinflammatory consequences and renal failure.

Detection of lesions in rRNA by primer extension analysis showed that the accumulated damage in 1x5 mice at 72 h was greater than that in 3x1 mice, suggesting that the development of Stx2-mediated renal failure may require an extended time to permit the animals to develop signs characteristic of HUS. In human disease, 10 to 15% of infected individuals progress to HUS 1 week after the initial onset of signs (1). Our results suggest that the administration of small, multiple injections of Stx2 may reproduce the development of HUS that occurs in humans over an extended period of time.

To determine whether administration of an anti-Stx2 Ab would prevent progression of HUS in our mouse model, we administered 11E10, a specific monoclonal Ab that recognizes the A subunit of Stx2, at various times after the second dose of 1 ng Stx2/20 g bwt. 3x1 mice receiving 11E10 on day 4 showed normal renal function and normal neutrophil and lymphocyte levels and lacked hemolysis at the time of sacrifice. In addition, these mice showed decreased fibrin(ogen) deposition compared to that of Stx-treated mice in the absence of Ab. The inflammatory response, as determined by measurement of proinflammatory transcripts in the kidney and demonstration of protein in the sera, was reduced by more than 50% in proinflammatory mRNAs and proteins that were examined. Taken together, these results indicate that passive immunization with anti-Stx2 Ab in mice was capable of preventing the lethality of the toxin, even after initial exposure to Stx and in the continued presence of circulating Stx.

Current treatment of HUS in patients is supportive, and effective therapeutic intervention has not been successful (1, 60). Our results suggest that passive immunization against Stx may be therapeutically effective in humans at risk of developing HUS, if Ab is able to be administered at an early time after development of signs and before the accumulated effects of HUS have resulted in irreversible structural damage.

ACKNOWLEDGMENTS

Supported by the National Institutes of Health (grants DK079419 [K.A.D.S.], ES889456 and AI1059335 [B.E.M.], and AI20148 [A.D.O.]).

REFERENCES

1. **Andreoli, S. P., H. Trachtman, D. W. Acheson, R. L. Siegler, and T. G. Obrig.** 2002. Hemolytic uremic syndrome: epidemiology, pathophysiology, and therapy. Pediatr. Nephrol. **17:**293–298.
2. **Baker, D. R., R. A. Moxley, and D. H. Francis.** 1997. Variation in virulence in the gnotobiotic pig model of O157:H7 Escherichia coli strains of bovine and human origin. Adv. Exp. Med. Biol. **412:**53–58.
3. **Barrett, T. J., M. E. Potter, and I. K. Wachsmuth.** 1989. Bacterial endotoxin both enhances and inhibits the toxicity of Shiga-like toxin II in rabbits and mice. Infect. Immun. **57:**3434–3437.
4. **Cherla, R. P., S. Y. Lee, P. L. Mees, and V. L. Tesh.** 2006. Shiga toxin 1-induced cytokine production is mediated by MAP kinase pathways and translation initiation factor eIF4E in the macrophage-like THP-1 cell line. J. Leukoc. Biol. **79:**397–407.
5. **Cohen, A., G. E. Hannigan, B. R. Williams, and C. A. Lingwood.** 1987. Roles of globotriosyl- and galabiosylceramide in verotoxin binding and high affinity interferon receptor. J. Biol. Chem. **262:**17088–17091.
6. **Dowling, T. C., P. A. Chavaillaz, D. G. Young, A. Melton-Celsa, A. O'Brien, C. Thuning-Roberson, R. Edelman, and C. O. Tacket.** 2005. Phase 1 safety and pharmacokinetic study of chimeric murine-human monoclonal antibody cαStx2 administered intravenously to healthy adult volunteers. Antimicrob. Agents Chemother. **49:**1808–1812.
7. **Drabkin, D. L.** 1971. Heme binding and transport—a spectrophotometric study of plasma glycoglobulin hemochromogens. Proc. Natl. Acad. Sci. USA **68:**609–613.
8. **Edwards, A. C., A. R. Melton-Celsa, K. Arbuthnott, S. J. R., C. K. Schmitt, H. C. Wong, and A. D. O'Brien.** 1998. Vero cell neutralization and mouse protective efficacy of humanized monoclonal antibodies against *Escherichia coli* toxins Stx1 and Stx2, p. 388–392. *In* J. B. Kaper and A. D. O'Brien (ed.), *Escherichia coli* O157:H7 and other Shiga toxin-producing *E. coli* strains. American Society for Microbiology, Washington, DC.
9. **Endo, Y., K. Mitsui, M. Motizuki, and K. Tsurugi.** 1987. The mechanism of action of ricin and related toxic lectins on eukaryotic ribosomes. The site and the characteristics of the modification in 28 S ribosomal RNA caused by the toxins. J. Biol. Chem. **262:**5908–5912.

10. **Endo, Y., and K. Tsurugi.** 1987. RNA N-glycosidase activity of ricin A-chain. Mechanism of action of the toxic lectin ricin on eukaryotic ribosomes. J. Biol. Chem. **262:**8128–8130.
11. **Endo, Y., K. Tsurugi, T. Yutsudo, Y. Takeda, T. Ogasawara, and K. Igarashi.** 1988. Site of action of a Vero toxin (VT2) from Escherichia coli O157:H7 and of Shiga toxin on eukaryotic ribosomes. RNA N-glycosidase activity of the toxins. Eur. J. Biochem. **171:**45–50.
12. **Foster, G. H., C. S. Armstrong, R. Sakiri, and V. L. Tesh.** 2000. Shiga toxin-induced tumor necrosis factor alpha expression: requirement for toxin enzymatic activity and monocyte protein kinase C and protein tyrosine kinases. Infect. Immun. **68:**5183–5189.
13. **Foster, G. H., and V. L. Tesh.** 2002. Shiga toxin 1-induced activation of c-Jun NH(2)-terminal kinase and p38 in the human monocytic cell line THP-1: possible involvement in the production of TNF-alpha. J. Leukoc. Biol. **71:** 107–114.
14. **Fujii, J., Y. Kinoshita, T. Yutsudo, H. Taniguchi, T. Obrig, and S. I. Yoshida.** 2001. Toxicity of Shiga toxin 1 in the central nervous system of rabbits. Infect. Immun. **69:**6545–6548.
15. **Gerber, A., H. Karch, F. Allerberger, H. M. Verweyen, and L. B. Zimmerhackl.** 2002. Clinical course and the role of Shiga toxin-producing Escherichia coli infection in the hemolytic-uremic syndrome in pediatric patients, 1997–2000, in Germany and Austria: a prospective study. J. Infect. Dis. **186:**493–500.
16. **Guessous, F., M. Marcinkiewicz, R. Polanowska-Grabowska, S. Kongkhum, D. Heatherly, T. Obrig, and A. R. Gear.** 2005. Shiga toxin 2 and lipopolysaccharide induce human microvascular endothelial cells to release chemokines and factors that stimulate platelet function. Infect. Immun. **73:**8306–8316.
17. **Habib, R.** 1992. Pathology of the hemolytic uremic syndrome, p. 315–353. *In* B. S. Kaplan (ed.), Hemolytic uremic syndrome and thrombotic thrombocytopenic purpura. Marcel Dekker, New York, NY.
18. **Hughes, A. K., P. K. Stricklett, D. Schmid, and D. E. Kohan.** 2000. Cytotoxic effect of Shiga toxin-1 on human glomerular epithelial cells. Kidney Int. **57:**2350–2359.
19. **Ikeda, M., S. Ito, and M. Honda.** 2004. Hemolytic uremic syndrome induced by lipopolysaccharide and Shiga-like toxin. Pediatr. Nephrol. **19:**485–489.
20. **Inward, C. D., A. J. Howie, M. M. Fitzpatrick, F. Rafaat, D. V. Milford, C. M. Taylor, et al.** 1997. Renal histopathology in fatal cases of diarrhoea-associated haemolytic uraemic syndrome. Pediatr. Nephrol. **11:**556–559.
21. **Iordanov, M. S., D. Pribnow, J. L. Magun, T. H. Dinh, J. A. Pearson, S. L. Chen, and B. E. Magun.** 1997. Ribotoxic stress response: activation of the stress-activated protein kinase JNK1 by inhibitors of the peptidyl transferase reaction and by sequence-specific RNA damage to the alpha-sarcin/ricin loop in the 28S rRNA. Mol. Cell. Biol. **17:**3373–3381.
22. **Karpman, D., H. Connell, M. Svensson, F. Scheutz, P. Alm, and C. Svanborg.** 1997. The role of lipopolysaccharide and Shiga-like toxin in a mouse model of Escherichia coli O157:H7 infection. J. Infect. Dis. **175:**611–620.
23. **Karpman, D., A. Hakansson, M. T. Perez, C. Isaksson, E. Carlemalm, A. Caprioli, and C. Svanborg.** 1998. Apoptosis of renal cortical cells in the hemolytic-uremic syndrome: in vivo and in vitro studies. Infect. Immun. **66:**636–644.
24. **Keepers, T. R., M. A. Psotka, L. K. Gross, and T. G. Obrig.** 2006. A murine model of HUS: Shiga toxin with lipopolysaccharide mimics the renal damage and physiologic response of human disease. J. Am. Soc. Nephrol. **17:**3404–3414.
25. **Kita, E., Y. Yunou, T. Kurioka, H. Harada, S. Yoshikawa, K. Mikasa, and N. Higashi.** 2000. Pathogenic mechanism of mouse brain damage caused by oral infection with Shiga toxin-producing *Escherichia coli* O157:H7. Infect. Immun. **68:**1207–1214.
26. **Kolling, G. L., F. Obata, L. K. Gross, and T. G. Obrig.** 2008. Immunohistologic techniques for detecting the glycolipid Gb(3) in the mouse kidney and nervous system. Histochem. Cell Biol. **130:**157–164.
27. **Korcheva, V., J. Wong, C. Corless, M. Iordanov, and B. Magun.** 2005. Administration of ricin induces a severe inflammatory response via nonredundant stimulation of ERK, JNK, and P38 MAPK and provides a mouse model of hemolytic uremic syndrome. Am. J. Pathol. **166:**323–339.
28. **Krautz-Peterson, G., S. Chapman-Bonofiglio, K. Boisvert, H. Feng, I. M. Herman, S. Tzipori, and A. S. Sheoran.** 2008. Intracellular neutralization of Shiga toxin 2 by an A subunit-specific human monoclonal antibody. Infect. Immun. **76:**1931–1939.
29. **Lingwood, C. A.** 1996. Role of verotoxin receptors in pathogenesis. Trends Microbiol. **4:**147–153.
30. **Lingwood, C. A., H. Law, S. Richardson, M. Petric, J. L. Brunton, S. De Grandis, and M. Karmali.** 1987. Glycolipid binding of purified and recombinant Escherichia coli produced verotoxin in vitro. J. Biol. Chem. **262:**8834–8839.
31. **Litalien, C., F. Proulx, M. M. Mariscalco, P. Robitaille, J. P. Turgeon, E. Orrbine, P. C. Rowe, P. N. McLaine, and E. Seidman.** 1999. Circulating inflammatory cytokine levels in hemolytic uremic syndrome. Pediatr. Nephrol. **13:**840–845.
32. **Mariani-Kurkdjian, P., and E. Bingen.** 1995. Hemolytic-uremic syndrome after verotoxin-producing Escherichia coli infection. Presse Med. **24:**99–101. (In French.)
33. **Melton-Celsa, A. R., and A. D. O'Brien.** 2000. Shiga toxins of Shigella dysenteriae and Escherichia coli. Handb. Exp. Pharmacol. **145:**385–406.
34. **Mukherjee, J., K. Chios, D. Fishwild, D. Hudson, S. O'Donnell, S. M. Rich, A. Donohue-Rolfe, and S. Tzipori.** 2002. Human Stx2-specific monoclonal antibodies prevent systemic complications of *Escherichia coli* O157:H7 infection. Infect. Immun. **70:**612–619.
35. **Mukherjee, J., K. Chios, D. Fishwild, D. Hudson, S. O'Donnell, S. M. Rich, A. Donohue-Rolfe, and S. Tzipori.** 2002. Production and characterization of protective human antibodies against Shiga toxin 1. Infect. Immun. **70:**5896–5899.
36. **Obrig, T. G., T. P. Moran, and J. E. Brown.** 1987. The mode of action of Shiga toxin on peptide elongation of eukaryotic protein synthesis. Biochem. J. **244:**287–294.
37. **O'Loughlin, E. V., and R. M. Robins-Browne.** 2001. Effect of Shiga toxin and Shiga-like toxins on eukaryotic cells. Microbes Infect. **3:**493–507.
38. **Palermo, M., F. Alves-Rosa, C. Rubel, G. C. Fernandez, G. Fernandez-Alonso, F. Alberto, M. Rivas, and M. Isturiz.** 2000. Pretreatment of mice with lipopolysaccharide (LPS) or IL-1beta exerts dose-dependent opposite effects on Shiga toxin-2 lethality. Clin. Exp. Immunol. **119:**77–83.
39. **Palermo, M. S., M. F. Alves Rosa, N. Van Rooijen, and M. A. Isturiz.** 1999. Depletion of liver and splenic macrophages reduces the lethality of Shiga toxin-2 in a mouse model. Clin. Exp. Immunol. **116:**462–467.
40. **Paton, J. C., and A. W. Paton.** 1998. Pathogenesis and diagnosis of Shiga toxin-producing *Escherichia coli* infections. Clin. Microbiol. Rev. **11:**450–479.
41. **Perera, L. P., L. R. Marques, and A. D. O'Brien.** 1988. Isolation and characterization of monoclonal antibodies to Shiga-like toxin II of enterohemorrhagic *Escherichia coli* and use of the monoclonal antibodies in a colony enzyme-linked immunosorbent assay. J. Clin. Microbiol. **26:**2127–2131.
42. **Proulx, F., E. G. Seidman, and D. Karpman.** 2001. Pathogenesis of Shiga toxin-associated hemolytic uremic syndrome. Pediatr. Res. **50:**163–171.
43. **Ray, P. E., and X. H. Liu.** 2001. Pathogenesis of Shiga toxin-induced hemolytic uremic syndrome. Pediatr. Nephrol. **16:**823–839.
44. **Richardson, S. E., T. A. Rotman, V. Jay, C. R. Smith, L. E. Becker, M. Petric, N. F. Olivieri, and M. A. Karmali.** 1992. Experimental verocytotoxemia in rabbits. Infect. Immun. **60:**4154–4167.
45. **Rovin, B. H., and L. T. Phan.** 1998. Chemotactic factors and renal inflammation. Am. J. Kidney Dis. **31:**1065–1084.
46. **Ruggenenti, P., M. Noris, and G. Remuzzi.** 2001. Thrombotic microangiopathy, hemolytic uremic syndrome, and thrombotic thrombocytopenic purpura. Kidney Int. **60:**831–846.
47. **Rutjes, N. W., B. A. Binnington, C. R. Smith, M. D. Maloney, and C. A. Lingwood.** 2002. Differential tissue targeting and pathogenesis of verotoxins 1 and 2 in the mouse animal model. Kidney Int. **62:**832–845.
48. **Sandvig, K.** 2001. Shiga toxins. Toxicon **39:**1629–1635.
49. **Saxena, S. K., A. D. O'Brien, and E. J. Ackerman.** 1989. Shiga toxin, Shiga-like toxin II variant, and ricin are all single-site RNA N-glycosidases of 28 S RNA when microinjected into Xenopus oocytes. J. Biol. Chem. **264:**596–601.
50. **Sheoran, A. S., S. Chapman, P. Singh, A. Donohue-Rolfe, and S. Tzipori.** 2003. Stx2-specific human monoclonal antibodies protect mice against lethal infection with *Escherichia coli* expressing Stx2 variants. Infect. Immun. **71:** 3125–3130.
51. **Sheth, K. J., H. M. Swick, and N. Haworth.** 1986. Neurological involvement in hemolytic-uremic syndrome. Ann. Neurol. **19:**90–93.
52. **Siegler, R. L., T. J. Pysher, R. Lou, V. L. Tesh, and F. B. Taylor, Jr.** 2001. Response to Shiga toxin-1, with and without lipopolysaccharide, in a primate model of hemolytic uremic syndrome. Am. J. Nephrol. **21:**420–425.
53. **Smith, W. E., A. V. Kane, S. T. Campbell, D. W. Acheson, B. H. Cochran, and C. M. Thorpe.** 2003. Shiga toxin 1 triggers a ribotoxic stress response leading to p38 and JNK activation and induction of apoptosis in intestinal epithelial cells. Infect. Immun. **71:**1497–1504.
54. **Suzuki, K., K. Tateda, T. Matsumoto, F. Gondaira, S. Tsujimoto, and K. Yamaguchi.** 2000. Effects of interaction between Escherichia coli verotoxin and lipopolysaccharide on cytokine induction and lethality in mice. J. Med. Microbiol. **49:**905–910.
55. **Taguchi, T., H. Uchida, N. Kiyokawa, T. Mori, N. Sato, H. Horie, T. Takeda, and J. Fujimoto.** 1998. Verotoxins induce apoptosis in human renal tubular epithelium derived cells. Kidney Int. **53:**1681–1688.
56. **Takahashi, K., N. Funata, F. Ikuta, and S. Sato.** 2008. Neuronal apoptosis and inflammatory responses in the central nervous system of a rabbit treated with Shiga toxin-2. J. Neuroinflammation **5:**11.
57. **Teel, L. D., J. A. Daly, R. C. Jerris, D. Maul, G. Svanas, A. D. O'Brien, and C. H. Park.** 2007. Rapid detection of Shiga toxin-producing *Escherichia coli* by optical immunoassay. J. Clin. Microbiol. **45:**3377–3380.
58. **Te Loo, D. M., V. W. van Hinsbergh, L. P. van den Heuvel, and L. A. Monnens.** 2001. Detection of verocytotoxin bound to circulating polymorphonuclear leukocytes of patients with hemolytic uremic syndrome. J. Am. Soc. Nephrol. **12:**800–806.
59. **Tesh, V. L., J. A. Burris, J. W. Owens, V. M. Gordon, E. A. Wadolkowski,**

A. D. O'Brien, and J. E. Samuel. 1993. Comparison of the relative toxicities of Shiga-like toxins type I and type II for mice. Infect. Immun. **61:**3392–3402.
60. **Tzipori, S., A. Sheoran, D. Akiyoshi, A. Donohue-Rolfe, and H. Trachtman.** 2004. Antibody therapy in the management of Shiga toxin-induced hemolytic-uremic syndrome. Clin. Microbiol. Rev. **17:**926–941.
61. **Upadhyaya, K., K. Barwick, M. Fishaut, M. Kashgarian, and N. J. Siegel.** 1980. The importance of nonrenal involvement in hemolytic-uremic syndrome. Pediatrics **65:**115–120.
62. **van Setten, P. A., V. W. van Hinsbergh, L. P. van den Heuvel, F. Preyers, H. B. Dijkman, K. J. Assmann, T. J. van der Velden, and L. A. Monnens.** 1998. Monocyte chemoattractant protein-1 and interleukin-8 levels in urine and serum of patents with hemolytic uremic syndrome. Pediatr. Res. **43:**759–767.
63. **Weiler-Guettler, H., P. D. Christie, D. L. Beeler, A. M. Healy, W. W. Hancock, H. Rayburn, J. M. Edelberg, and R. D. Rosenberg.** 1998. A targeted point mutation in thrombomodulin generates viable mice with a prethrombotic state. J. Clin. Investig. **101:**1983–1991.
64. **Yamagami, S., M. Motoki, T. Kimura, H. Izumi, T. Takeda, Y. Katsuura, and Y. Matsumoto.** 2001. Efficacy of postinfection treatment with anti-Shiga toxin (Stx) 2 humanized monoclonal antibody TMA-15 in mice lethally challenged with Stx-producing Escherichia coli. J. Infect. Dis. **184:**738–742.

Editor: B. A. McCormick